GLIA 55:954–965 (2007)

# Caspase-3 Activation in Astrocytes Following Postnatal Excitotoxic Damage Correlates With Cytoskeletal Remodeling but not With Cell Death or Proliferation

LAIA ACARIN,[1]* SONIA VILLAPOL,[1] MARYAM FAIZ,[1] TROY T. ROHN,[2] BERNARDO CASTELLANO,[1] AND BERTA GONZÁLEZ[1]
[1]*Medical Histology, Department of Cell Biology, Physiology and Immunology, Faculty of Medicine and Institute of Neurosciences, Autonomous University of Barcelona, Spain*
[2]*Department of Biology, Boise State University, Boise, Idaho*

*KEY WORDS*
immature; astrogliosis; cytoskeleton; caspase

*ABSTRACT*
Caspase-3 has classically been defined as the main executioner of programmed cell death. However, recent data supports the participation of this protease in non-apoptotic cellular events including cell proliferation, cell cycle regulation, and cellular differentiation. In this study, astroglial cleavage of caspase-3 was analyzed following excitotoxic damage in postnatal rats to determine if its presence is associated with apoptotic cell death, cell proliferation, or cytoskeletal remodeling. A well-characterized *in vivo* model of excitotoxicity was studied, where damage was induced by intracortical injection of *N*-methyl-D-asparate (NMDA) in postnatal day 9 rats. Our results demonstrate that cleaved caspase-3 was mainly observed in the nucleus of activated astrocytes in the lesioned hemisphere as early as 4 h postlesion and persisted until the glial scar was formed at 7–14 days, and it was not associated with TUNEL labeling. Caspase-3 enzymatic activity was detected at 10 h and 1 day postlesion in astrocytes, and co-localized with caspase-cleaved fragments of glial fibrillary acidic protein (CCP-GFAP). However, at longer survival times, when astroglial hypertrophy was observed, astroglial caspase-3 did not generally correlate with GFAP cleavage, but instead was associated with *de novo* expression of vimentin. Moreover, astroglial caspase-3 cleavage was not associated with BrdU incorporation. These results provide further evidence for a nontraditional role of caspases in cellular function that is independent of cell death and suggest that caspase activation is important for astroglial cytoskeleton remodeling following cellular injury. 

## INTRODUCTION

Caspase-3 is considered one of the major executioners of apoptosis and has classically been viewed as a terminal event in the process of programmed cell death. Caspase-3 is proteolytically activated into two catalytic subunits of 10 kDa (p10) and 20 kDa (p20), which can cleave numerous intracellular substrates including cytoskeletal elements, degrading proteases, and nuclear enzymes involved in DNA repair (Marks and Berg, 1999; Springer et al., 2001) to name just a few. Accordingly, caspase-3 activation has been described in neuronal cells following specific types of central nervous system (CNS) insults including traumatic brain injury and ischemic/excitotoxic damage (Beer et al., 2000; Brecht et al., 2001; Chen et al., 1998; Manabat et al., 2003; Namura et al., 1998; Nath et al., 2000; Pulera et al., 1998). In all of these conditions, the participation of executioner caspase activation and subsequent apoptosis in the neuronal cell death process has largely been established both in the adult and postnatal brain. Similarly, *in vitro* studies have also suggested that caspase-3 proteolytic activity plays a crucial role in excitotoxin-induced neuronal apoptosis (Allen et al., 1999; Du et al., 1997; Tenneti and Lipton, 2000), although caspase-3 activation and DNA fragmentation often do not co-localize within the same cell at the same time (Brecht et al., 2001). In addition, expression of caspase-3 has been described in oligodendrocytes (Beer et al., 2000; Nottingham and Springer, 2003) and astrocytes following CNS damage (Beer et al., 2000; Benjelloun et al., 2003; Mouser et al., 2006; Narkilahti et al., 2003; Su et al., 2000).

Recent studies, however, provide substantial evidence for caspase function in non-apoptotic cellular events such as cell cycle regulation, migration, and differentiation in a variety of cell types (McLaughlin, 2004; Schwerk and Schulze-Osthoff, 2003). Although the preponderance of data has emerged from work in the immune system and peripheral organs, several studies have also suggested non-apoptotic roles of caspase-3 in the CNS. Under physiological conditions, caspase-3 has been implicated in neuronal cytoskeletal changes (Rohn et al., 2004), in synaptic remodeling (Dash et al., 2000; Shimohama et al., 2001), in neuronal survival associated with preconditioning (Garnier et al. 2003; McLaughlin et al., 2003; Tanaka et al., 2004), in the differentiation of cerebellar Bergmann glial cells (Oomman et al., 2004, 2005, 2006), and as a marker of astroglial subpopulations

Grant sponsor: Ministry of Education and Science; Grant number: BFU2005-02783, 2005SGR-00956.

*Correspondence to: Laia Acarin, Medical Histology, Torre M5, Faculty of Medicine, Universitat Autonoma Barcelona, Bellaterra 08193 (Barcelona), Spain. E-mail: Laia.acarin@uab.es

Received 22 December 2006; Accepted 10 April 2007

DOI 10.1002/glia.20518

Published online 8 May 2007 in Wiley InterScience (www.interscience.wiley.com).

(Noyan-Ashraf et al., 2005). Accordingly, following excitotoxic damage in the neonatal brain we have demonstrated that presence of cleaved caspase-3 in nitrated reactive astrocytes in the absence of cell death (Acarin et al., 2005). Nevertheless, alternative roles for caspase-3 in CNS astrocytes after injury have not been described.

The first aim of the present study was to describe the pattern, time course, and cellular distribution of cleaved caspase-3 and TUNEL labeling after postnatal excitotoxicity by using a well characterized *in vivo* lesion model in the immature rat brain (Acarin et al., 1999a,b, 2002, 2005). Brain damage as a consequence of perinatal cerebral hypoxia/ischemia and stroke is a major cause of acute mortality and severe chronic disabilities, and excitotoxicity is one of the crucial underlying mechanisms. Several evidences suggest that in comparison to the adult brain, the immature brain responds in a particular fashion to brain injuries, partly due to the fact that many of adult gene expression patterns, neural circuits organization, cell differentiation, and myelination have not yet been completed (Ferriero, 2004; Vannucci and Hagberg, 2004). Furthermore, as astroglial cells were the main cell type showing cleaved caspase-3 but not apoptotic cell death after neonatal excitotoxicity, the second aim was to elucidate the putative role that caspase-3 may play in proliferation and cytoskeletal reorganization in reactive astrocytes. Our findings suggest a participation of this protease in astroglial remodeling of intermediate filaments containing glial fibrillary acidic protein (GFAP) and vimentin after damage, more so than a contribution to cell death or modulation of proliferation.

## MATERIALS AND METHODS

### Excitotoxic Lesions

Nine-day-old Long-Evans black-hooded rat pups of both sexes were placed in a stereotaxic frame adapted for newborns (Kopf) under isofluorane anaesthesia. The skull was opened using a surgical blade, and 0.15 μL of saline solution (0.9% NaCl, pH 7.4) containing 20 nmols of *N*-methyl-D-aspartate (NMDA) (Sigma, M-3262, Germany) were injected into the right sensorimotor cortex. Control animals received an injection of 0.15 μL of the vehicle saline solution. After suture, pups were placed in a thermal pad and maintained at normothermia before being returned to their mothers. Experimental animal work was conducted according to Spanish regulations, in agreement with European Union directives. All experimental procedures were approved by the ethical commission of the Autonomous University of Barcelona. All efforts were made to minimize animal suffering.

### Survival Times and Sample Processing

Rats were sacrificed at 4 and 10 h and 1, 3, 5, 7, and 14 days after NMDA or saline injection. For histological procedures, rats were anesthetized by ether inhalation and perfused intracardially with 4% paraformaldehyde in 0.1 M phosphate buffer (pH 7.4). Brains were post-fixed in the same fixative for 2 h and sunk in a 30% sucrose solution before being frozen with dry $CO_2$. Coronal sections (30-μm-thick) were obtained using a Leitz cryostat. For caspase-3 activity, rats were sacrificed by decapitation, brains were quickly removed and the cortices dissected out, frozen in liquid nitrogen and kept at −80°C. A minimum of four NMDA-injected animals, two saline-injected controls, and two intact controls were used for each survival time and each procedure.

### 5′-Bromodeoxyuridine Administration

In another set of animals, the thymidine analogue 5′-bromodeoxyuridine (BrdU, Sigma Chemical, St Louis, MO) that incorporates into the DNA of dividing cells during S-phase, was used to label actively proliferating cells. NMDA or saline injected animals were administered intraperitonealy with BrdU (50 mg/kg) diluted in 0.05 M Tris base (TB, pH 7.4) every 2 h for 10 h before sacrifice at 1, 3, 5, and 7 days after NMDA or saline injection.

### Immunohistochemistry and Histochemistry

After rinsing for 1 h in 0.05 M tris-buffered saline (TBS), endogenous peroxidase was blocked with 2% $H_2O_2$ in 70% methanol for 10 min. Sections were rinsed in TBS and TBS + 1% triton X-100 and incubated in blocking buffer (BB, TBS containing 10% FCS, and 1% triton X-100) for 30 min. The sections were then incubated overnight at 4°C and 1 h at room temperature with either primary rabbit anti-cleaved caspase-3 (recognizing the p17/19 kDa fragment, 1:200, Cell Signaling Technology, 9661) or primary rabbit anti-cleaved caspase-3 (recognizing the p17 subunit, 1:600, R&D Systems, AF835) in BB. After washing, sections were incubated for 1 h at room temperature with a biotin-conjugated anti-rabbit secondary antibody (1:200, RPN1004, Amersham Pharmacia), rinsed in TBS + 1% triton and incubated for 1 h at room temperature with HRP-conjugated streptavidin (1:400, PO364, Dakopatts). Finally, the peroxidase reaction product was visualized by incubating the sections in 100 mL of TB containing 50 mg 3,3′diaminobenzidine (DAB) and 33 μL hydrogen peroxide. As negative controls for immunohistochemistry, sections were incubated in media lacking primary antibody.

Double staining procedures were used for the simultaneous visualization of cleaved caspase-3 and NeuN as a neuronal marker; GFAP and vimentin as astroglial markers; Adenomatus Polyposis Coli (APC) as a marker for oligodendrocytes, GFAP-CCP as a marker of caspase-cleaved GFAP, BrdU as a marker for proliferating cells, and tomato lectin histochemistry to label microglial cells. For double fluorescent labeling, sections were processed for cleaved caspase-3 labeling as described

earlier but using a Cy3-conjugated anti-rabbit secondary antibody (1:1,000; PA4300V, Amersham Pharmacia). Afterwards, sections were incubated overnight at 4°C and 1 h at room temperature in either monoclonal mouse anti-NeuN (1:1,000; MAB377, Chemicon); polyclonal rabbit anti-GFAP (1:1,800; Z-0224, Dakopatts); monoclonal mouse anti-vimentin (1:1,000; M0725, Dakopatts); monoclonal mouse anti-APC (CC-1) (1:500, OP80, Calbiochem); monoclonal mouse anti-BrdU (1:80, B5002, Dakopatts); or polyclonal rabbit anti-CCP-GFAP (Mouser et al., 2006) diluted in BB. Sections were then washed in TBS + 1% triton X-100 and incubated for 1 h at room temperature with either Cy2-conjugated anti-rabbit secondary antibody (1:1,000; PA-42004, Amersham Pharmacia) or Cy2-conjugated anti-mouse secondary antibody (1:1,000; PA42002, Amersham Pharmacia). For tomato lectin histochemistry, sections were incubated for 2 h at 37° in tomato lectin (1:150, L0651, Sigma) in TBS + 1% triton X-100. After washing, sections were incubated for 1 h at room temperature with Cy2-conjugated avidin (1:1,000; PA-42000, Amersham Pharmacia). Selected mounted sections were stained with a fluorescent nuclear marker by incubating slides for 10 min in a DAPI (D9542, Sigma) solution at a concentration of 0.00125 μg/mL. After washing, sections were dehydrated, air-dried, and cover-slipped using DPX. Fluorescence and light microscopy digital images were captured with a Nikon Digital Eclipse DXM1200 color camera attached to a Nikon E-800 microscope. Confocal images were obtained using a LEICA TCS SP2 AOBS confocal microscope.

### Terminal dUTP Nick End Labeling (TUNEL) Staining and Double Labeling with Cleaved Caspase-3, and Neuronal and Glial Markers

For TUNEL staining, tissue sections were rinsed in Tris buffer (10 mM, pH 8) and EDTA (5 mM) and then incubated in the same buffer plus Proteinase K (20 μg/mL) for 15 min at room temperature. After several washes with EDTA (5 mM), sections were incubated for 10 min in TdT buffer (Tris 30 mM, 140 mM sodium cacodilate, 1 mM cobalt chloride, pH 7,7). Sections were then incubated in TdT buffer plus 0.161 U/μL TdT enzyme (Terminal Transferase, 3333566 Roche, Manheim, Germany) and 0.0161 nmol/μL of biotin-16-dUTP (1093070, Roche, Manheim, Germany) for 30 min at 37°C. The reaction was stopped by washing the sections in citrate buffer (300 mM sodium chloride, 30 mM sodium citrate, 5 mM EDTA). After several washes with TBS, sections were incubated with HRP-conjugated streptavidin (1:400, SA5004, Vector Laboratories) and the peroxidase reaction product was visualized in a solution containing 0.02% DAB, 2.4% nickel ammonium, 0.04% chloride ammonium, 0.2% glucose D+, and 0.0027% glucose oxidase in 0.1 M acetate buffer (pH 6.0).

For double labeling, TUNEL-stained sections were incubated with either anti-NeuN, anti-GFAP, anti-APC, or tomato lectin as described in the previous section but using biotin-conjugated secondary antibodies: biotin-conjugated anti-rabbit secondary antibody (1:200, RPN1004, Amersham) for GFAP or biotin-conjugated anti-mouse secondary antibody (1:200, RPN1001, Amersham) for NeuN and APC and incubated for 1 h at room temperature with HRP-conjugated streptavidin (1:400, PO364 Dakopatts). Sections incubated with tomato lectin were directly incubated in the HRP-conjugated streptavidin (1:400, PO364 Dakopatts). Finally, peroxidase reaction product was visualized by incubating the slides in 100 mL of tris buffer containing 50 mg DAB and 33 μL of hydrogen peroxide.

For TUNEL fluorescent labeling and double immunostaining with cleaved caspase-3, free-floating sections were first incubated with the primary antibody anti-cleaved caspase-3 (1:1,000; Cell Signaling Technology, 9661), which was visualized by using Cy3-conjugated anti-rabbit secondary antibody (1:1,000; PA-42004, Amersham). Afterwards, sections were mounted on slides and TUNEL labeling was performed as described above but using Cy2-conjugated streptavidin (1:1,000; PA-42000, Amersham Pharmacia) to visualize the staining.

### Caspase-3 Activity Assay

Ipsilateral cortices of intact controls, saline-injected, and NMDA-injected animals, were weighed and homogenized in ice-cold Tris/HCl buffer containing a cocktail of protease inhibitors. Homogenates were centrifuged (12,000 rpm) for 10 min at 4°C and supernatants were extracted and assayed for caspase-3 activity using EnzCheck assay kit #1 containing Z-DEVD-AMC substrate (E-13183 Molecular Probes, Invitrogene), following Manufacturer's instructions. Caspase activity was measured in 50 μL of sample for 30 min using a fluorimeter at 340/360 nm of excitation and 440/460 nm emission, using appropriate filters. Arbitrary fluorescent units were converted into micromoles of AMC release using a standard curve and standardized to total protein in each sample. Enzyme activity is shown as micromolar AMC released/mg total protein. As a control, the protease inhibitor Ac-DVED-CHO was incubated with alternate samples and controls to inhibit caspase-3-like activity.

### Cell Number Quantification

Digital images were captured at different magnifications with a Nikon Digital Eclipse DXM1200 color camera attached to a Nikon E-800 microscope using the software ACT-1 2.20 (Nikon Corporation). TUNEL-positive cells, cleaved caspase-3-positive cells, and cleaved caspase-3/GFAP double positive cells were counted in 20× micrographs from the cortical lesion core. For the analysis of TUNEL-GFAP double-labeled cells, TUNEL-positive and double TUNEL/GFAP-positive cells of the same area were counted in micrographs taken at 40× from the cortical lesion core. In all cell counts, at least 10 consecutive sections were counted for each animal and averaged.

A minimum of three animals for each survival time were used.

### Data Processing and Statistical Analysis

All results are expressed as mean ± standard error mean (SEM). Statistical analysis was performed using StatView software, where differences were evaluated by one-way analysis of variance (ANOVA) followed by Fisher's PLSD *post-hoc* test comparisons to determine significant differences ($P < 0.05$) between survival times and cell types.

## RESULTS

Injection of the excitotoxin NMDA into the right sensorimotor cortex of postnatal day 9 rat pups caused a lesion involving neuronal loss and a glial response in the entire thickness of the cortex and the dorsal striatum at the level of the injection site, which has been previously described in detail (Acarin et al., 1996; 1999a,b, 2000a). Injection of a control saline solution resulted in slight tissue disruption restricted to the area of the needle track and a focal and transient glial response that lasted until three days postinjection.

### Distribution and Time Course of Cleaved Caspase-3 Immunoreactivity and Caspase-3 Enzymatic Activity

Cleaved caspase-3 immunoreactivity in both intact control and saline-injected brains, was seen in the ventricle walls and meninges and in cells accumulated in the cingulum of the corpus callosum (Fig. 1B). In contrast, in NMDA-injected animals, cleaved caspase-3-positive cells were found in the ipsilateral hemisphere at all survival times examined. Both primary antibodies used for the detection of cleaved caspase-3 (see methods section) showed similar results. Cleaved caspase-3 labeling was commonly found in the nuclei, and in a minority of cells in the perinuclear region (Fig. 1). At 4 h postlesion, scattered cleaved caspase-3-positive cells were present in the damaged cortex (Figs. 1A,C), mainly in the periphery of the degenerating area. At 10 h and 1 day postlesion, extensive dark cleaved caspase-3 staining was seen throughout the degenerating cortical area, namely in the upper cortical layers and the medial cortex, and in the ipsilateral dorsal striatum (Figs. 1D–F). The maximum number of cleaved caspase-3-positive cells in the neurodegenerating cortex was seen at day 1 (Fig. 2), when fainter caspase staining was also observed in adjacent cortex and the corpus callosum. At days 3 and 5, cleaved caspase-3 staining was still evident in the cortical neurodegenerative area (Figs. 1G–I) but the number of positive cells was slightly diminished (Fig. 2). In addition, cleaved caspase-3-positive cells were also present in the dorsal striatum, and in the deeper cortical layer VI even at caudal levels far from the lesioned area (Fig. 1G). From day 7, the number of positive cells was clearly reduced and cleaved caspase-3 immunoreactivity became restricted to the glial scar, with darker staining observed in the upper cortical layers and fainter staining in the lower cortical layers and corpus callosum (Figs. 1J–L and 2).

The analysis of caspase-3 activity using a fluorimetric assay showed no differences within the different postnatal ages, both in intact controls and in saline-injected controls. However, NMDA-injected cortices showed significant enzymatic caspase-3 activity at 10 h and 1 day postlesion, but this activity was not significantly different from controls at shorter or longer survival times (Fig. 3).

### Identification of Cleaved Caspase-3 Positive Cells by Double Labeling with Specific Cellular Markers

In control animals and in the contralateral hemispheres of lesioned animals, cleaved caspase-3-positive cells were identified as GFAP-positive astroglial cells in the cingulum of the corpus callosum (data not shown). In the damaged hemisphere of lesioned animals, cleaved caspase-3 was seen both in neurons and astrocytes (see Fig. 4). Mainly at 10 h and 1 day postlesion, cleaved caspase-3 immunolabeling was observed in NeuN-positive neuronal cells within the degenerating core and in the proximal lesion border (Figs. 4A,B), but not in the distant caudal cortex (Fig. 4C). Cleaved caspase-3 labeling in neurons was both nuclear and cytoplasmic (Figs. 1E,F and 4B).

Colocalization of cleaved caspase-3 in the nuclei of astroglial cells was evident in the damaged cortex and the adjacent corpus callosum from 4 h postlesion, the first survival time analyzed (Figs. 4D and 5). At 10 h postlesion, when a decrease in GFAP immunoreactivity is observed in the lesion core (Acarin et al., 1999b), double-labeled cleaved caspase-3/GFAP-positive astrocytes comprised 35% of the total number of cleaved caspase-3-positive cells, the lowest percentage seen at all time points examined (see Fig. 5). At day 1 postlesion, the presence of cleaved caspase-3 was associated with astroglial hypertrophy and increased GFAP labeling (Figs. 4E,F) and by the onset of vimentin expression (Acarin et al., 1999b). Astrocytes in cortical layer VI and in the striatum showed stronger cleaved caspase-3 immunoreactivity than those located in the corpus callosum. From 3 days postlesion, astrocytes were the main population showing cleaved caspase-3 immunoreactivity (see Fig. 5). At this time and at 5 days postlesion, increased GFAP immunoreactivity and astroglial hypertrophy was observed throughout the neurodegenerative area. The observed astroglial hypertrophy was also associated with vimentin immunoreactivity as well as the presence of cleaved caspase-3 in the nucleus (Figs. 4G–H). From 7 days postlesion, reactive hypertrophied astrocytes located in the glial scar showed cleaved caspase-3 immunoreactivity in the nucleus and strong GFAP (Fig. 4I) and vimentin labeling.

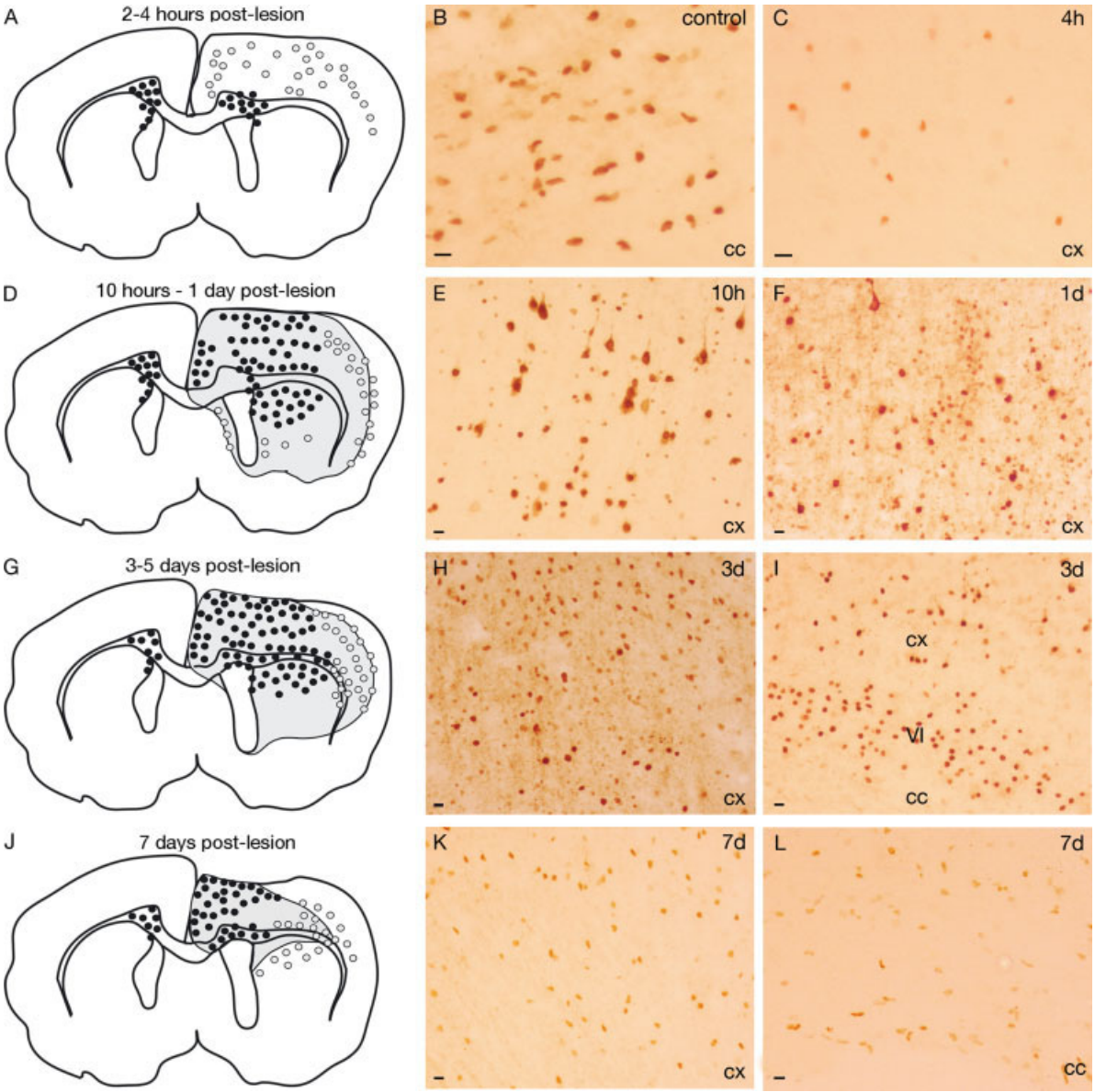


Fig. 1. Temporal and spatial distribution of cleaved caspase-3 immunoreactive cells at different survival times following a cortical excitotoxic lesion in the immature brain. Lesioned area is encircled and shown in light grey in the ipsilateral right hemisphere from 10 h post-lesion (**D**, **G**, **J**). Cells strongly labeled for cleaved caspase-3 are shown in black circles, whereas mildly positive cells are depicted in white circles. In the contralateral control hemisphere cleaved caspase-3 cells are found in the cingulum of the corpus callsoum (left hemisphere in **A**, **B**). In NMDA-injected ipsilateral hemisphere, immunoreactive cells are seen in the cortex and corpus callosum at all survival times (**A**–**L**). cc, corpus callosum; cx, cortex; VI, cortical layer VI. Scale bars = 10 μm. [Color figure can be viewed in the online issue, which is available at www.interscience.wiley.com.]

We did not find, at any survival time, colocalization between cleaved caspase-3 immunoreactivity and tomato lectin, a specific marker for either microglia/macrophages or endothelial cells (Fig. 4J). In addition, colocalization was not evident between cleaved caspase-3 and the APC-positive oligodendrocytes (Figs. 4K–L).

### Association Between Cleaved Caspase-3 and Proliferation

To assess the role of caspase-3 in cellular proliferation, the cleavage of caspase-3 was examined in BrdU positive cells in animals injected with the thymidine analogue prior to sacrifice. Few BrdU-positive cells showed cleaved caspase-3 labeling in the nucleus, while the majority of cleaved caspase-3 labeled nuclei did not show BrdU incorporation at any survival times studied (Figs. 6A,B).

### Association Between Cleaved Caspase-3 and the Presence of Caspase-Cleaved GFAP Fragments

Presence of cleaved caspase-3 in astrocytes was associated with the presence of caspase-cleaved GFAP fila-

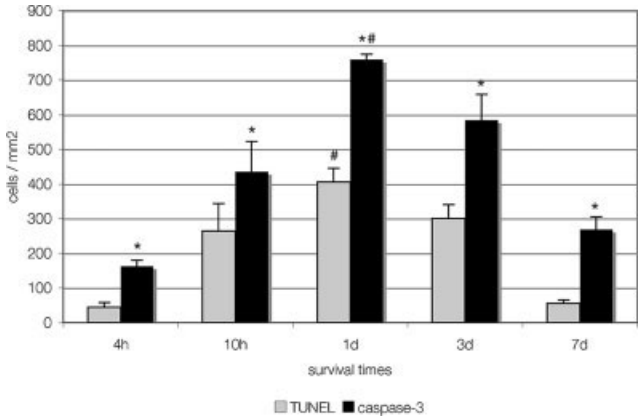


Fig. 2. Quantification of cleaved caspase-3 positive cells and TUNEL positive cells in the excitotoxically injured cortex of postnatal rats at different survival times ($n = 4$ for each labeling and survival time). Cleaved caspase-3-positive cells outnumber TUNEL-positive cells at all survival times ($^*P < 0.05$). Maximum density of both cleaved caspase-3-positive cells and TUNEL-positive cells is seen at day 1 postlesion ($^{\#}P < 0.05$).

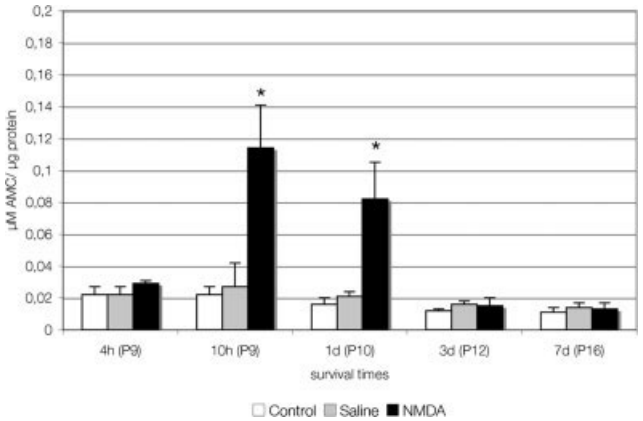


Fig. 3. Caspase-3 enzymatic activity in the cortex of intact control postnatal rats of 9 days of age (P9), P10, P12, P14, and P16 ($n = 2$ for each age); and at different survival times following saline ($n = 2$ for each survival time) or NMDA-injection ($n = 4$ for each survival time). Caspase-3 enzymatic activity is significant at 10 h and 1 day postlesion in NMDA-injected cortex ($^*P < 0.05$) in comparison to both control and lesioned cortices at 4 h, 3 or 7 days postlesion, when caspase-3 activity was not different from controls.

ments by using a recently described site-directed caspase-cleavage antibody specific to GFAP, termed CCP-GFAP (Mouser et al., 2006). CCP-GFAP immunostaining was located within the lesion core from 10 h until the last survival time examined, peaking at day 1. At 10 h and 1 day postlesion, CCP-GFAP was observed as rounded beads in the cytoplasm of astrocytes, which displayed cleaved caspase-3 in their nuclei (Figs. 6E–H) and were located in the lesion core and immediately surrounding cortex (Fig. 6E). Interestingly, GFAP immunoreactivity was markedly reduced in those cell projections showing CCP-GFAP immunolabeling (Figs. 6F–G). At day 3 postlesion, only scattered reactive astrocytes showed CCP-GFAP within the GFAP-positive filaments (Fig. 6H), and were mainly located in the medial cortex and the upper cortical layers. No association at all was found at 7 days between CCP-GFAP and GFAP (Fig. 6I), and instead CCP-GFAP-positive structures were located within lectin-labeled macrophages (data not shown).

## Association Between Cleaved Caspase-3 and TUNEL Labeling

Saline-injection in controls resulted in only a few number of TUNEL-positive cells, being located primarily in the region of the needle track, where tissue disruption occurs, and occasionally in the meninges. In NMDA-injected animals, TUNEL-positive nuclei displaying condensed chromatin, pyknotic nuclei, or apoptotic bodies were seen from 10 h until 7 days postlesion. Quantitative analysis revealed a maximum number of TUNEL-positive cells at 1 day postlesion and decreasing thereafter (see Fig. 2). TUNEL-positive apoptotic cells were located in the cortical lesion site but also extended to the dorsal striatum, the septum, and CA fields of the rostral hippocampus, but were rarely found in the corpus callosum. In general, cleaved caspase-3-positive nuclei always outnumbered those showing TUNEL-labeling at all times examined (see Fig. 2). Although some cells showed both cleaved caspase-3 and TUNEL staining, many cleaved caspase-3-positive cells did not colocalize with TUNEL and furthermore, many TUNEL-positive cells did not display cleaved caspase-3 labeling (Figs. 6C,D).

## Double Labeling for TUNEL and Specific Cell Markers

Qualitatively, we could observe that most TUNEL-positive cells observed at all time points postlesion were identified as NeuN-positive neuronal cells (Figs. 7A,B) and that TUNEL/NeuN double labeled cells were more frequent than cleaved caspase-3/NeuN double positive cells (compare with Figs. 4A–C). TUNEL-positive neurons often showed nuclear fragmentation (Fig. 7A) and were located in the cortical degenerating area (Figs. 7A,B), cortical layer VI, the dorsal striatum, and the rostral hippocampus CA field (data not shown).

In addition, although most lectin-positive microglial cells did not show TUNEL labeling (Fig. 7C), some microglia/macrophages with characteristic round or ameboid phagocytic forms at 5 days postlesion were found (Fig. 7D).

Analysis of TUNEL/GFAP double-labeled sections showed few astrocytes with TUNEL-positive nuclei, contrasting with the high presence of cleaved caspase-3 in reactive astrocytes. At 10 h, when massive TUNEL staining was observed in neuronal cells, only 8% of all TUNEL-positive cells were astrocytes (Fig. 5). These cells were found close to the tissue disrupted at the site of the needle track, and in the corpus callosum (Figs. 7E–F). At days 3–5, although astrocytes did not gener-

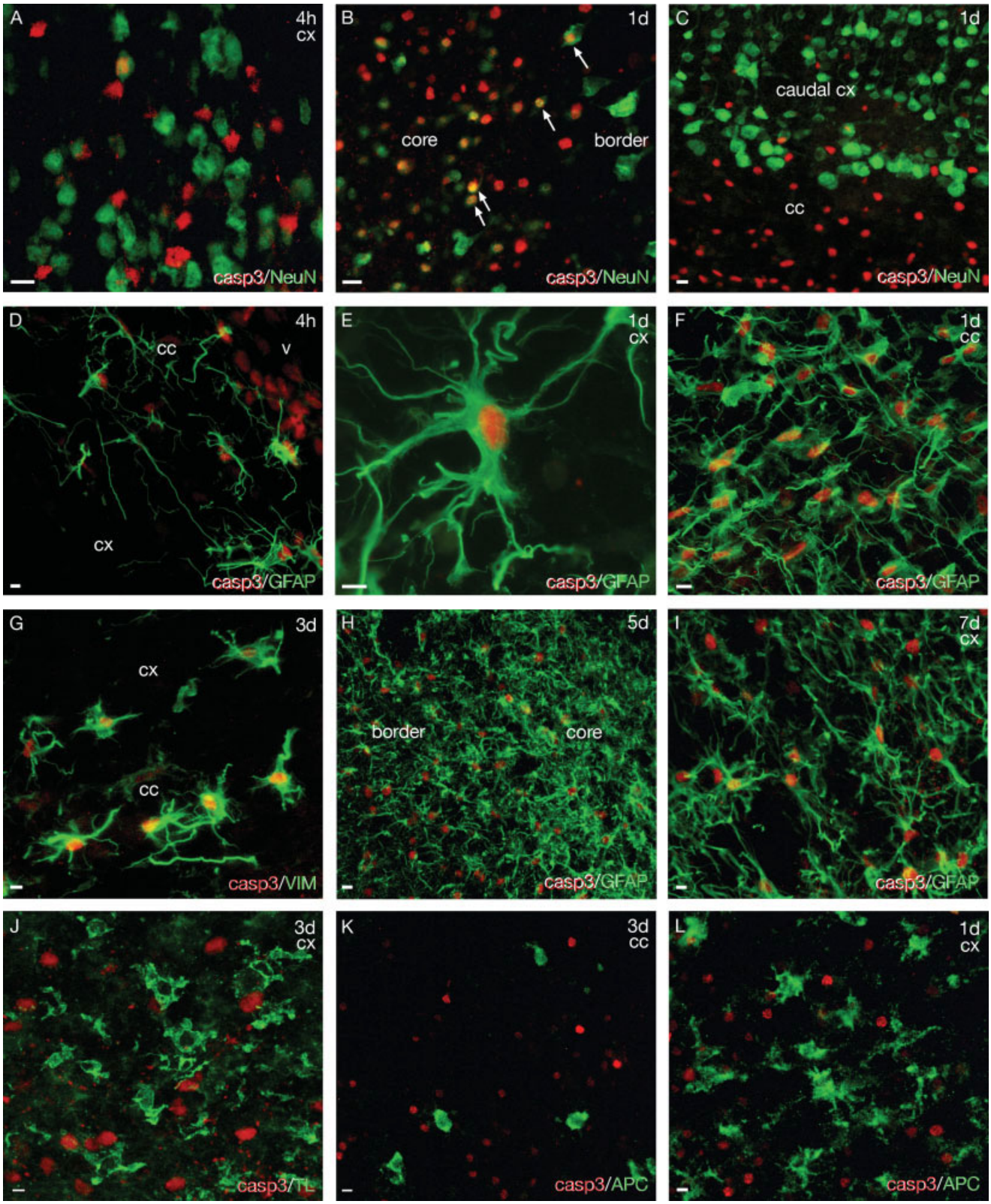


Fig. 4. Identification of cleaved caspase-3-positive cells at different survival times following a cortical excitotoxic lesion in the postnatal brain. Caspase-3 (casp3) labeling is shown in red, whereas the neuronal marker NeuN (in **A**–**C**), the astroglial markers GFAP (in **D**–**F**, **H**, and **I**) and vimentin (VIM) (in **G**), the microglial marker tomato lectin (TL) (in **J**), and the oligodendroglial marker APC (in **K** and **L**) are shown in green. NeuN-positive neuronal cells do not generally show cleaved caspase-3 labeling at 4 h postlesion (A), but labeling is seen in neurons at 10 h and 1 day postlesion (arrows in B) in the lesion core and the proximal border (B) but not in the distal caudal cortex (c). In contrast, astrocytes show nuclear cleaved caspase-3 as early as 4 h postlesion (D) and persists until the last survival time analyzed (I). Cleaved caspase-3 positive astrocytes are seen in the corpus callosum (cc) (F), the lesion core and cortical border (H) and in the cortical glial scar (I). Cleaved caspase-3 colocalizes with vimentin-positive astrocytes (G). In contrast, no TL-positive cells (J) or APC-positive oligodendrocyte (K, L) show cleaved caspase-3 labeling. cc, corpus callosum; cx, cortex; v, ventricle. Scale bars = 10 μm. [Color figure can be viewed in the online issue, which is available at www.interscience.wiley.com.]

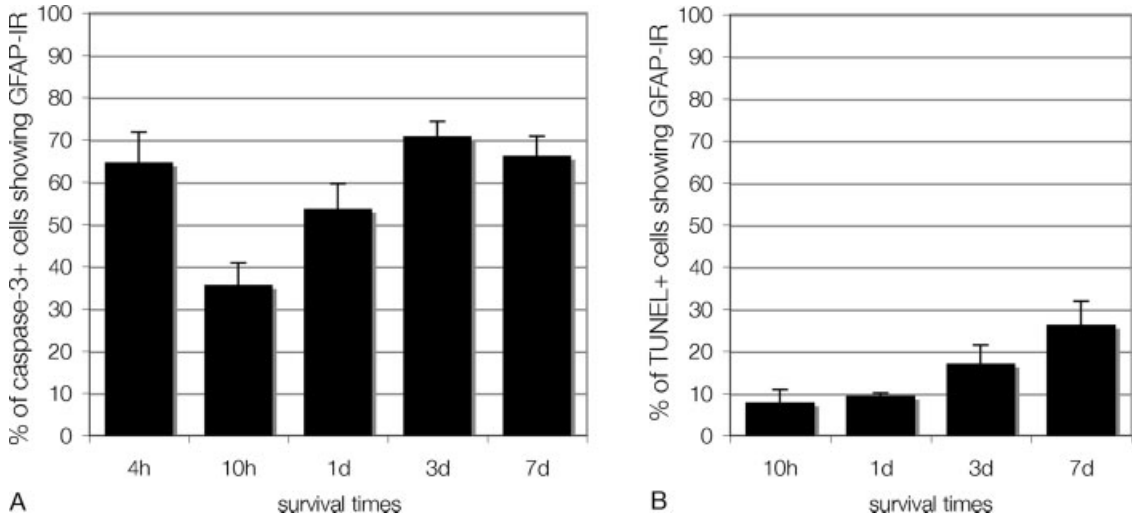


Fig. 5. Quantification of cleaved caspase-3/GFAP (**A**) and TUNEL/GFAP (**B**) double positive cells in the excitotoxically damaged cortex at different survival times. Data are shown as the percentage of cleaved caspase-3 positive cells showing GFAP colocalization (A) ($n = 4$ for each survival time), and percentage of TUNEL positive cells showing GFAP colocalisation (B) ($n = 3$ for each survival time). GFAP-positive astrocytes are the majority of cleaved caspase-3 positive cells at 4 h and 3–7 days postlesion (A). Lower percentages are found at 10 h and 1 day postlesion. Decreased immunoreactivity for GFAP within the lesion core (see results) found at these times may account for the reduction in the amount of double positive cells. In contrast, GFAP/TUNEL-positive cells are a minority of TUNEL-positive cells at all survival times. However, percentage increases with time and in the cortical glial scar at 7 days postlesion, when the densitiy of TUNEL-positive cells at this timepoint is strongly diminished (see Fig. 2), GFAP/TUNEL-positive account for 26% of all TUNEL-positive nuclei. IR, immunoreactivity.

ally show TUNEL-positive nuclei, reactive astrocytes were frequently seen surrounding TUNEL-positive nuclei with their projections (Figs. 7G–I). At longer survival times, TUNEL staining was strongly reduced and was not found in the majority of scar forming GFAP-positive astrocytes (Fig. 7J). However, some reactive astrocytes located in the upper and more superficial glial scar and in the medial cortex showed TUNEL-positive nuclei (Figs. 7K–L), representing 26% of the total number of TUNEL-positive cells identified (Fig. 5). It should be noted that the number of TUNEL-positive cells at this time is strongly reduced (Fig. 2). Analysis of double-labeling for TUNEL and the oligodendroglial marker APC showed few if any TUNEL-positive oligodendrocytes throughout all survival times analyzed (Fig. 7M).

## DISCUSSION

This study shows that following excitotoxic cortical damage to the postnatal rat brain, cleaved caspase-3 can be observed in some neuronal cells, the main cell type undergoing apoptotic cell death, as classicaly reported. However, the majority of cleaved caspase-3 was found in the nuclei of activated astrocytes within the lesioned hemisphere from early times and until glial scar formation. Neither microglial cells nor oligodendrocytes showed cleaved caspase-3 immunoreactivity. Interestingly, astroglial caspase-3 cleavage did not generally correlate with TUNEL labeling and apoptotic astrocytes were only seen at specific times and regions.

Astroglial cells can undergo cell death *in vitro* in a variety of situations such as calcium overload, oxidative stress, mitochondrial dysfunction, and treatment with apoptotic inducers like staurosporine and ceramide (Giffard and Swanson, 2005; Takuma et al., 2004), although it has been established that they are more resistant than neuronal cells (Xu et al., 2004). In this regard, studies of astroglial cell death after different types of acute injuries such as traumatic brain injury (Beer et al., 2000; Newcomb et al., 1999) and ischemia/excitotoxicity (Biran et al., 2006; Dihne et al., 2001), have shown that apoptosis occurs only in few astrocytes, in agreement with our findings in the injured neonatal brain. Alternatively, non-apoptotic roles of caspase-3 need to be considered.

### Cleaved Caspase-3 is Found in the Astroglial Nuclei

The nuclear localization of cleaved caspase-3 in astrocytes has not only been previously demonstrated in injury paradigms (Acarin et al., 2005; Benjelloun et al., 2003; Johnson et al., 2005), but also in astrocytes of the normal adult CNS (Noyan-Ashraf et al., 2005) and in differentiating Bergmann glial cells (Oomman et al., 2005). It is largely established that during apoptosis, caspase-3 is the main protease responsible for the cleavage of nuclear proteins, like Poly(ADP-ribose) Polymerase-1 (PARP-1), acinus, and lamins (Eldadah and Faden, 2000), inducing DNA damage and chromatin condensation. To date, however, very little is known about the function of caspase-cleaved nuclear proteins that are independent of apoptosis, but recent reports have suggested several possible mechanisms. First, caspase-generated

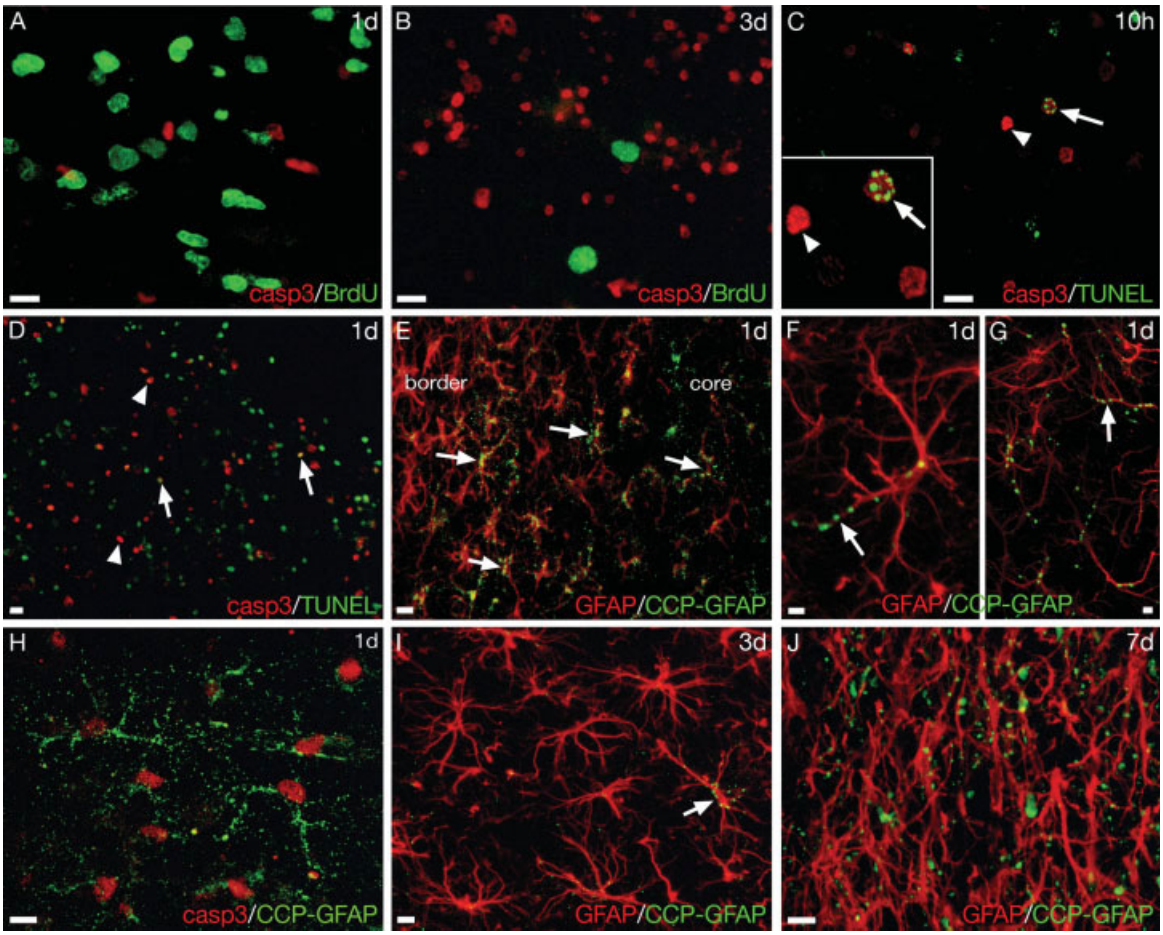


Fig. 6. Colocalization of cleaved caspase-3 with BrdU, TUNEL, and CCP-GFAP immunolabeling at several days (d) postlesion. Cleaved caspase-3 (casp3) (**A**-**D** and **H**) and GFAP (**E**-**G**, **I**, and **J**) are shown in red. BrdU (A, B), TUNEL (C, D), and CCP-GFAP (E-J) are shown in green. No colocalization is observed between cleaved caspase-3 and BrdU incorporation (A, B). Colocalization between cleaved caspase-3 and TUNEL labeling is seen in some cells (arrows in C and D), but TUNEL-negative and cleaved caspase-3-positive cells are more frequent (arrowheads in C and D). At 10 h and 1 day postlesion CCP-GFAP is seen in GFAP-positive astrocytes in the lesion core and adjacent border (arrows in E). CCP-GFAP shows a beaded immunoreactivity associated to astroglial projections which usually display low GFAP content (arrows in F and G). CCP-GFAP colocalizes with cleaved caspase-3 labeling within the lesion core (H). At 3 days, CCP-GFAP labeling is clearly diminished and only few immunoreactive astrocytes remain (arrow in I). No colocalization is seen at longer survival times (J). Scale bars = 10 μm. [Color figure can be viewed in the online issue, which is available at www.interscience.wiley.com.]

fragments of PARP-1 can interact with Nuclear Factor kappa B (NFkappaB) subunits and enhance NFkappaB transcriptional activity (Lamkanfi et al., 2006), a transcription factor present in the nucleus of postnatal reactive astrocytes (Acarin et al., 2000b). Second, cleavage of FoxO transcription factors, like FoxO3a, that contain a conserved caspase-3 cleavage site (Charvet et al., 2003), could also play a role in the modulation of gene expression during glial differentiation or astrogliosis. Third, it has been suggested that caspase-3 could serve as a mechanism of protein degradation required for the cellular response to changes in extrinsic signals (McLaughlin, 2004).

### Presence of Caspase-Cleaved GFAP

One of the main findings of the present study was the detection of beaded caspase-cleaved GFAP immunoreactivity in astrocytes, colocalizing with cleaved caspase-3, within the lesion core at 10–24 h postlesion, when caspase-3 enzymatic activity was observed. Decreased GFAP immunoreactivity induced by excitotoxicity and ischemia within the lesion core during the first 24 h postlesion is a well characterized event, both in the immature (Acarin et al., 1999b), adult (Dihne et al., 2001), and aged brain (Castillo-Ruiz et al., 2007). As caspase-generated GFAP fragments are not recognized by commonly used GFAP antibodies directed to the full length molecule (Mouser et al., 2006), caspase-mediated cleavage of GFAP could, at least in part, explain the decrease in GFAP immunoreactivity observed in the lesion core at early times in several injury paradigms. This decrease in GFAP, together with the existence of astrocytes showing low GFAP content in gray matter (Walz, 2000), obviously leads an underestimation of the number of GFAP-positive astrocytes showing caspase-3 at early times (see Fig. 5).

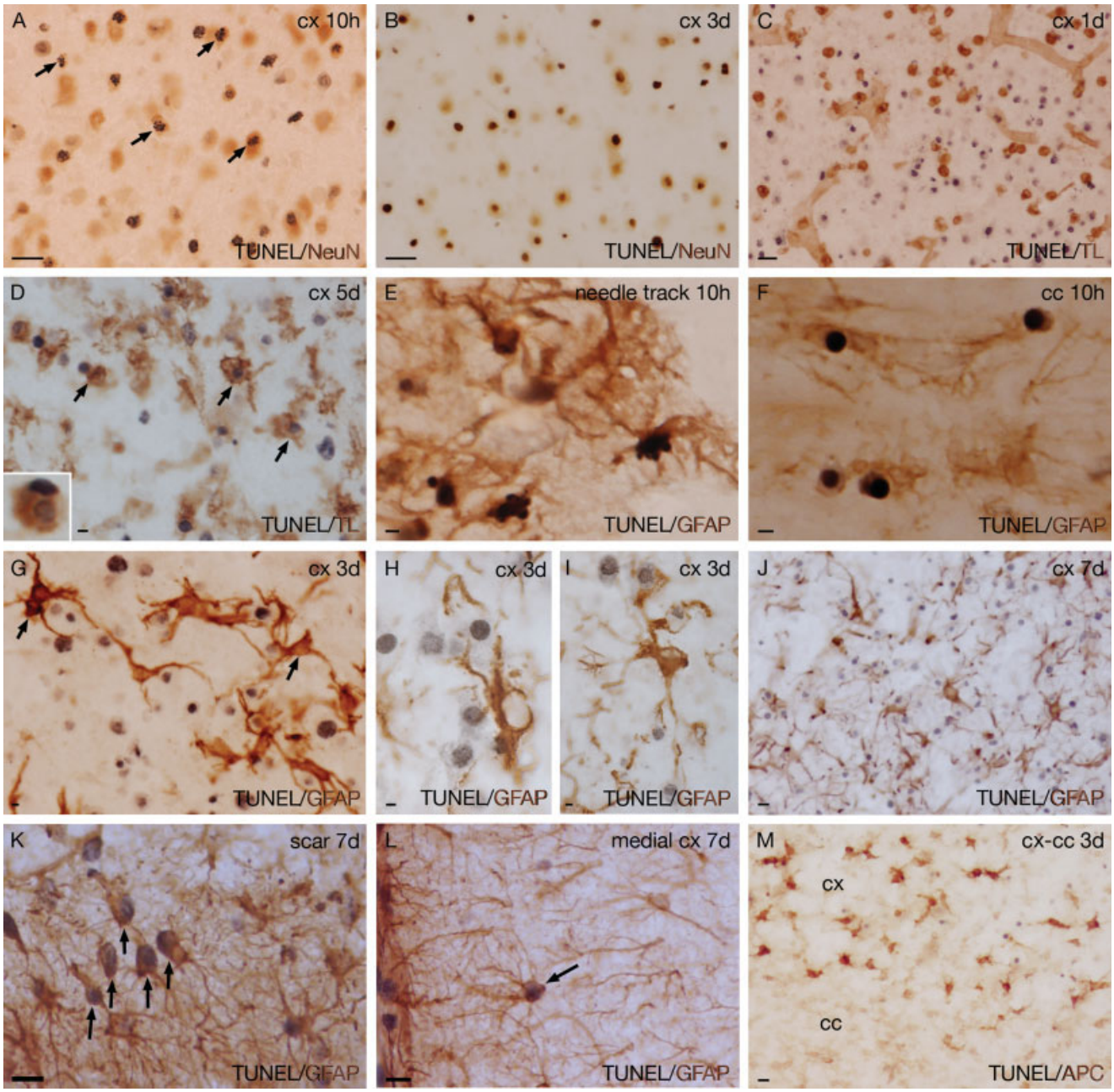


Fig. 7. Identification of TUNEL-positive cells at different survival times following a cortical excitotoxic lesion. TUNEL labeling is shown in gray-black (**A**-**M**) and NeuN (A, B), Tomato lectin (TL) (C, D), GFAP (E-L), or APC (M) are shown in brown. The majority of TUNEL-positive cells show NeuN labeling at different survival times (A, B). At 10 h and 1 day postlesion, TUNEL/NeuN double positive cells commonly display fragmented nuclei (arrows in A). Double staining for TUNEL and TL shows that whereas no colocalization is found at early times (C), some macrophages at 5–7 days postlesion display TUNEL-positive nuclei and/or TUNEL-positive material within the cytoplasm (inset in D). In TUNEL/GFAP double labeled sections, scattered double positive cells are found at 10 h in the needle track (E) and adjacent corpus callosum (F). At days 1–5 postlesion, no double positive cells are found (G-J), although close proximity between processes of GFAP-positive astrocytes and TUNEL-positive nuclei is often observed (arrows in G and H, I). At longer survival times, in the glial scar, scattered astrocytes located in the upper cortical layers (arrows in K) and the medial cortex (arrow in L) do show TUNEL-positive nuclei. No colocaization is seen between TUNEL and the oligodendroglial marker APC (M). Cc, corpus callosum; cx, cortex. Scale bars = 10 μm. [Color figure can be viewed in the online issue, which is available at www.interscience.wiley.com.]

In Alzheimer' disease brain (AD) and mouse models of AD, caspase-cleaved GFAP colocalizes with cleaved caspase-3 in beaded and/or fragmented processes of astrocytes located in plaque-rich regions and near blood vessels (Mouser et al., 2006), a process thought to be associated with cytoskeletal dismantling and cell death. However, in this model of acute postnatal injury, it is unclear if cleavage of GFAP is associated with cell death or contributes to cytoskeletal remodeling and associative morphological changes. In this regard, it should be noted that from 3 days postlesion, cleaved caspase-3 was found in hypertrophied reactive astrocytes that did not immu-

nolabelled for caspase-cleaved GFAP. Therefore, an interesting hypothesis would be that caspase-3 is participating in astrocyte cytoskeletal remodeling processes, a characteristic feature of astrogliosis, by cleaving intermediate filament proteins at specific sites. In support of this, we found that a majority of the reactive astrocytes expressing vimentin also were positive for cleaved caspase-3. Vimentin is specifically cleaved by caspase-3, irreversibly dismantling intermediate filaments (Byun et al., 2001), which may impact the integrity and dynamics of intracellular structures (Morishima, 1999). Similarly, the GFAP sequence contains a single caspase consensus sequence, $DLTD^{266}$, based on the general tetrapeptide motif DXXD recognized by caspases, and the antibody CCP-GFAP used in this study was synthesized to the downstream neoepitope that would be generated after caspase cleavage of full length GFAP (Mouser et al., 2006).

### Other Non-Apoptotic Roles of Caspase-3

An important conclusion of this study is that cleaved caspase-3 is found in surviving reactive astrocytes, supporting the hypothesis of a non-apoptotic role of astroglial cleaved caspase-3, as has been postulated in other cell types, where non-apoptotic activities of caspases include the regulation of cell proliferation and differentiation (for review see McLaughlin, 2004; Schwerk and Schulze-Osthoff, 2003). One of the first described non-apoptotic roles of caspase-3 was the demonstration that caspase-3 cleavage is a physiological step during T lymphocyte activation and mitogenic induction (Miossec et al., 1997; Wilhelm et al., 1998). Recently, caspase-3 was characterized as a cell cycle-regulated protein considered a mitotic check point in HeLa cells (Hsu et al., 2006).

In the CNS, caspase activation may also play a role in neuronal cell dispersion and correct morphology (Rohn et al., 2004), and non-apoptotic neuronal caspase-3 cleavage occurs during normal hippocampal neuronal function such as in long-term potentiation processes (Dash et al., 2000), and in the soma and nerve endings of the adult brain, suggesting a contribution of this caspase to the regulation of synaptic plasticity (Shimohama et al., 2001). In addition, caspase-3 activation and substrate cleavage has been reported in the absence of cell death in gerbil hypoxia (Garnier et al., 2004) and in ischemic tolerance where neuronal caspase-3 is essential for the neuroprotective effect of preconditioning (Garnier et al. 2003; McLaughlin et al., 2003; Tanaka et al., 2004). Furthermore, other studies have also demonstrated a role of caspase-3 in the maturation of cerebellar granular cells during development (Oomman et al., 2004) and the differentiation of neural progenitor cells in the olfactory bulb (Fernando et al., 2005; Yan et al., 2001). Progenitor cells that divide and migrate through the rostral migratory stream en route to the olfactory bulb, show cleaved caspase-3 but no signs of cell death (Yan et al., 2001). In the present study, despite the fact that astroglial cells do undergo proliferation in this model of postnatal excitotoxicity (unpublished findings) no association was found between nuclear caspase-3 and BrdU incorporation.

With regards to glial cell differentiation, Oomann and coworkers, who have described cleaved caspase-3 in Bergmann glia during postnatal development in the absence of apoptotic or proliferation markers, have demonstrated a role of this protease in differentiation processes (Oomman et al., 2004, 2005, 2006). In addition, it was recently shown that constitutive non-apoptotic expression of the cleaved form of caspase-3 occurs in the nuclei of a subpopulation of astrocytes in the cerebellar cortex, hippocampus, and spinal cord of adult rats of different strains, which show expression of the sodium dependent glutamate transporter (EAAT1, GLAST) (Noyan-Ashraf et al., 2005). In relation to this, it was recently reported that the other glutamate transporter EAAT2, also expressed predominantly in astrocytes, is cleaved by caspase-3, leading to a drastic and selective inhibition of the transporter (Boston-Howes et al., 2006). In view of all these findings, it is becoming evident that caspase-3 may have unique, nontraditional roles in astrocytes that may be important to determine changes in cell phenotyping either during differentiation or after injury.

In conclusion, this study demonstrates for the first time that immature brain damage causes astroglial caspase-3 cleavage without associated apoptotic death. Alternative roles for capase 3 were examined, but no correlation was seen between caspase-3 and cell proliferation. Instead, this work suggests a novel role for cleaved caspase-3 in the cytoskeletal remodeling associated with astrogliosis.

## ACKNOWLEDGMENTS

We would like to thank M.A. Martil for his excellent technical help, E. Sanz for helping in the activity assay, and M. Roldan from the Servei Microscopia for confocal microscopy assistance. SV and MF hold a FI fellowship from the Autonomous University of Barcelona, Spain.

## REFERENCES

Acarin L, Gonzalez B, Castellano B. 2000a. Neuronal, astroglial and microglial cytokine expression after an excitotoxic lesion in the immature rat brain. Eur J Neurosci 12:3505–3520.

Acarin L, Gonzalez B, Castellano B. 2000b. STAT3 and NFkappaB activation precedes glial reactivity in the excitotoxically injured young cortex but not in the corresponding distal thalamic nuclei. J Neuropathol Exp Neurol 59:151–163.

Acarin L, Gonzalez B, Castellano B, Castro AJ. 1996. Microglial response to N-methyl-D-aspartate-mediated excitotoxicity in the immature rat brain. J Comp Neurol 367:361–374.

Acarin L, González B, Castro AJ, Castellano B. 1999a. Primary cortical glial reaction versus secondary thalamic glial response in the excitotoxically injured young brain. Microglial/macrophage response and MHC class I, II expression. Neuroscience 89:549–565.

Acarin L, González B, Hidalgo J, Castro AJ, Castellano B. 1999b. Primary cortical glial reaction versus secondary thalamic glial response in the excitotoxically injured young brain. Astroglial response and metallothionein expression. Neuroscience 92:827–839.

Acarin L, Peluffo H, Barbeito L, Castellano B, Gonzalez B. 2005. Astroglial nitration after postnatal excitotoxic damage: Correlation with nitric oxide sources, cytoskeletal, apoptotic and antioxidant proteins. J Neurotrauma 22:189–200.

Acarin L, Peluffo H, Gonzalez B, Castellano B. 2002. Expression of inducible nitric oxide synthase and cyclooxygenase-2 after excitotoxic damage to the immature rat brain. J Neurosci Res 68:745–754.

Allen JW, Knoblach SM, Faden AI. 1999. Combined mechanical trauma and metabolic impairment in vitro induces NMDA receptor-dependent neuronal cell death and caspase-3-dependent apoptosis. Faseb J 13:1875–1882.

Beer R, Franz G, Srinivasan A, Hayes RL, Pike BR, Newcomb JK, Zhao X, Schmutzhard E, Poewe W, Kampfl A. 2000. Temporal profile and cell subtype distribution of activated caspase-3 following experimental traumatic brain injury. J Neurochem 75:1264–1273.

Benjelloun N, Joly LM, Palmier B, Plotkine M, Charriaut-Marlangue C. 2003. Apoptotic mitochondrial pathway in neurones and astrocytes after neonatal hypoxia-ischaemia in the rat brain. Neuropathol Appl Neurobiol 29:350–360.

Biran V, Joly LM, Heron A, Vernet A, Vega C, Mariani J, Renolleau S, Charriaut-Marlangue C. 2006. Glial activation in white matter following ischemia in the neonatal P7 rat brain. Exp Neurol 199:103–112.

Boston-Howes W, Gibb SL, Williams EO, Pasinelli P, Brown RH Jr, Trotti D. 2006. Caspase-3 cleaves and inactivates the glutamate transporter EAAT2. J Biol Chem 281:14076–14084.

Brecht S, Gelderblom M, Srinivasan A, Mielke K, Dityateva G, Herdegen T. 2001. Caspase-3 activation and DNA fragmentation in primary hippocampal neurons following glutamate excitotoxicity. Brain Res Mol Brain Res 94:25–34.

Byun Y, Chen F, Chang R, Trivedi M, Green KJ, Cryns VL. 2001. Caspase cleavage of vimentin disrupts intermediate filaments and promotes apoptosis. Cell Death Differ 8:443–450.

Castillo-Ruiz MM, Campuzano O, Acarin L, Castellano B, Gonzalez B. 2007. Delayed neurodegeneration and early astrogliosis after excitotoxicity to the aged brain. Exp Gerontol 42:343–354.

Charvet C, Alberti I, Luciano F, Jacquel A, Bernard A, Auberger P, Deckert M. 2003. Proteolytic regulation of Forkhead transcription factor FOXO3a by caspase-3-like proteases. Oncogene 22:4557–4568.

Chen J, Nagayama T, Jin K, Stetler RA, Zhu RL, Graham SH, Simon RP. 1998. Induction of caspase-3-like protease may mediate delayed neuronal death in the hippocampus after transient cerebral ischemia. J Neurosci 18:4914–4928.

Dash PK, Blum S, Moore AN. 2000. Caspase activity plays an essential role in long-term memory. Neuroreport 11:2811–2816.

Dihne M, Block F, Korr H, Topper R. 2001. Time course of glial proliferation and glial apoptosis following excitotoxic CNS injury. Brain Res 902:178–189.

Du Y, Bales KR, Dodel RC, Hamilton-Byrd E, Horn JW, Czilli DL, Simmons LK, Ni B, Paul SM. 1997. Activation of a caspase 3-related cysteine protease is required for glutamate-mediated apoptosis of cultured cerebellar granule neurons. Proc Natl Acad Sci USA 94: 11657–11662.

Eldadah BA, Faden AI. 2000. Caspase pathways, neuronal apoptosis, and CNS injury. J Neurotrauma 17:811–29.

Fernando P, Brunette S, Megeney LA. 2005. Neural stem cell differentiation is dependent upon endogenous caspase 3 activity. Faseb J 19:1671–1673.

Ferriero DM. 2004. Neonatal brain injury. N Engl J Med 351:1985–1995.

Garnier P, Prigent-Tessier A, Van Hoecke M, Bertrand N, Demougeot C, Sordet O, Swanson RA, Marie C, Beley A. 2004. Hypoxia induces caspase-9 and caspase-3 activation without neuronal death in gerbil brains. Eur J Neurosci 20:937–946.

Garnier P, Ying W, Swanson RA. 2003. Ischemic preconditioning by caspase cleavage of poly (ADP-ribose) polymerase-1. J Neurosci 23: 7967–73.

Giffard RG, Swanson RA. 2005. Ischemia-induced programmed cell death in astrocytes. Glia 50:299–306.

Hsu SL, Yu CT, Yin SC, Tang MJ, Tien AC, Wu YM, Huang CY. 2006. Caspase 3, periodically expressed and activated at G2/M transition, is required for nocodazole-induced mitotic checkpoint. Apoptosis 11:765–771.

Johnson EA, Svetlov SI, Wang KK, Hayes RL, Pineda JA. 2005. Cell-specific DNA fragmentation may be attenuated by a survivin-dependent mechanism after traumatic brain injury in rats. Exp Brain Res 167:17–26.

Lamkanfi M, Declercq W, Vanden Berghe T, Vandenabeele P. 2006. Caspases leave the beaten track: Caspase-mediated activation of NF-kappaB. J Cell Biol 173:165–171.

Manabat C, Han BH, Wendland M, Derugin N, Fox CK, Choi J, Holtzman DM, Ferriero DM, Vexler ZS. 2003. Reperfusion differentially induces caspase-3 activation in ischemic core and penumbra after stroke in immature brain. Stroke 34:207–213.

Marks N, Berg MJ. 1999. Recent advances on neuronal caspases in development and neurodegeneration. Neurochem Int 35:195–220.

McLaughlin B. 2004. The kinder side of killer proteases: Caspase activation contributes to neuroprotection and CNS remodeling. Apoptosis 9:111–121.

McLaughlin B, Hartnett KA, Erhardt JA, Legos JJ, White RF, Barone FC, Aizenman E. 2003. Caspase 3 activation is essential for neuroprotection in preconditioning. Proc Natl Acad Sci USA 100:715–720.

Miossec C, Dutilleul V, Fassy F, Diu-Hercend A. 1997. Evidence for CPP32 activation in the absence of apoptosis during T lymphocyte stimulation. J Biol Chem 272:13459–13462.

Morishima N. 1999. Changes in nuclear morphology during apoptosis correlate with vimentin cleavage by different caspases located either upstream or downstream of Bcl-2 action. Genes Cells 4:401–414.

Mouser PE, Head E, Ha KH, Rohn TT. 2006. Caspase-mediated cleavage of glial fibrillary acidic protein within degenerating astrocytes of the Alzheimer's disease brain. Am J Pathol 168:936–946.

Namura S, Zhu J, Fink K, Endres M, Srinivasan A, Tomaselli KJ, Yuan J, Moskowitz MA. 1998. Activation and cleavage of caspase-3 in apoptosis induced by experimental cerebral ischemia. J Neurosci 18: 3659–3668.

Narkilahti S, Pirttila TJ, Lukasiuk K, Tuunanen J, Pitkanen A. 2003. Expression and activation of caspase 3 following status epilepticus in the rat. Eur J Neurosci 18:1486–1496.

Nath R, Scott M, Nadimpalli R, Gupta R, Wang KK. 2000. Activation of apoptosis-linked caspase(s) in NMDA-injured brains in neonatal rats. Neurochem Int 36:119–126.

Newcomb JK, Zhao X, Pike BR, Hayes RL. 1999. Temporal profile of apoptotic-like changes in neurons and astrocytes following controlled cortical impact injury in the rat. Exp Neurol 158:76–88.

Nottingham SA, Springer JE. 2003. Temporal and spatial distribution of activated caspase-3 after subdural kainic acid infusions in rat spinal cord. J Comp Neurol 464:463–471.

Noyan-Ashraf MH, Brandizzi F, Juurlink BH. 2005. Constitutive nuclear localization of activated caspase 3 in subpopulations of the astroglial family of cells. Glia 49:588–593.

Oomman S, Finckbone V, Dertien J, Attridge J, Henne W, Medina M, Mansouri B, Singh H, Strahlendorf H, Strahlendorf J. 2004. Active caspase-3 expression during postnatal development of rat cerebellum is not systematically or consistently associated with apoptosis. J Comp Neurol 476:154–173.

Oomman S, Strahlendorf H, Dertien J, Strahlendorf J. 2006. Bergmann glia utilize active caspase-3 for differentiation. Brain Res 1078:19–34.

Oomman S, Strahlendorf H, Finckbone V, Strahlendorf J. 2005. Non-lethal active caspase-3 expression in Bergmann glia of postnatal rat cerebellum. Brain Res Dev Brain Res 160:130–45.

Pulera MR, Adams LM, Liu H, Santos DG, Nishimura RN, Yang F, Cole GM, Wasterlain CG. 1998. Apoptosis in a neonatal rat model of cerebral hypoxia-ischemia. Stroke 29:2622–2630.

Rohn TT, Cusack SM, Kessinger SR, Oxford JT. 2004. Caspase activation independent of cell death is required for proper cell dispersal and correct morphology in PC12 cells. Exp Cell Res 295:215–225.

Schwerk C, Schulze-Osthoff K. 2003. Non-apoptotic functions of caspases in cellular proliferation and differentiation. Biochem Pharmacol 66:1453–1458.

Shimohama S, Tanino H, Fujimoto S. 2001. Differential subcellular localization of caspase family proteins in the adult rat brain. Neurosci Lett 315:125–128.

Springer JE, Nottingham SA, McEwen ML, Azbill RD, Jin Y. 2001. Caspase-3 apoptotic signaling following injury to the central nervous system. Clin Chem Lab Med 39:299–307.

Su JH, Nichol KE, Sitch T, Sheu P, Chubb C, Miller BL, Tomaselli KJ, Kim RC, Cotman CW. 2000. DNA damage and activated caspase-3 expression in neurons and astrocytes: Evidence for apoptosis in frontotemporal dementia. Exp Neurol 163:9–19.

Takuma K, Baba A, Matsuda T. 2004. Astrocyte apoptosis: implications for neuroprotection. Prog Neurobiol 72:111–127.

Tanaka H, Yokota H, Jover T, Cappuccio I, Calderone A, Simionescu M, Bennett MV, Zukin RS. 2004. Ischemic preconditioning: neuronal survival in the face of caspase-3 activation. J Neurosci 24:2750–2759.

Tenneti L, Lipton SA. 2000. Involvement of activated caspase-3-like proteases in N-methyl-D-aspartate-induced apoptosis in cerebrocortical neurons. J Neurochem 74:134–142.

Vannucci SJ, Hagberg H. 2004. Hypoxia-ischemia in the immature brain. J Exp Biol 207(Part 18):3149–3154.

Walz W. 2000. Controversy surrounding the existence of discrete functional classes of astrocytes in adult gray matter. Glia 31:95–103.

Wilhelm S, Wagner H, Hacker G. 1998. Activation of caspase-3-like enzymes in non-apoptotic T cells. Eur J Immunol 28:891–900.

Xu L, Chock VY, Yang EY, Giffard RG. 2004. Susceptibility to apoptosis varies with time in culture for murine neurons and astrocytes: Changes in gene expression and activity. Neurol Res 26:632–643.

Yan XX, Najbauer J, Woo CC, Dashtipour K, Ribak CE, Leon M. 2001. Expression of active caspase-3 in mitotic and postmitotic cells of the rat forebrain. J Comp Neurol 433:4–22.